Intermetallic σ and π Communication in Heterodinuclear μ-Cyclooctatetraene Complexes**

Gerdjan Bögels, Hugo C. Brussaard, Ute Hagenau, Jürgen Heck,* Jürgen Kopf, Johannes G. M. van der Linden, and Annie Roelofsen

Dedicated to Professor Gottfried Huttner on the occasion of his 60th birthday

Abstract: The reaction of $[(C_5R_5)Cr(\eta^6\text{-Cot})]$ (R = H, Me; Cot = cyclooctatetraene) with $[(CO)_3Fe(\eta\text{-}cis\text{-cyclooctene})_2]$ affords the heterodinuclear complexes $[(C_5R_5)Cr\{\mu\text{-}\eta^5(Cr):\eta^3(Fe)\text{-Cot}\}Fe(CO)_3]$ (R = H: **1**, R = Me: **2**) in quite good yields. One of the CO ligands in **1** and **2** can be easily substituted by a phosphane ligand, PR'_3 (R′ = Me, Ph, OEt, F) to obtain $[(C_5R_5)Cr\{\mu\text{-}\eta^5(Cr):\eta^3(Fe)\text{-Cot}\}Fe(CO)_2PR'_3]$ (R = H, R′ = Me: **3a**; R = H, R′ = Ph: **3b**; R = Me, R′ = Me: **4a**; R = Me, R′ = Ph: **4b**; R = Me, R′ = OEt: **4c**; R = Me, R′ = F: **4d**). The X-ray structure determinations of **2**, **3a**, and **4c** showed exclusively synfacial coordination of the two metal ligand moieties, despite the bulky C_5Me_5 (Cp*) ligand in **2** and **4c**. However, the steric demand of Cp* gives rise to structural distortions in **2** and **4c**, compared to the Cp-containing products **1** and **3a**, and an elongation of the Cr–Fe distance from 293 pm to 303 and 304 pm, respectively. The heterodinuclear complexes were investigated by cyclic voltammetry and ESR spectroscopy in order to elucidate the role of the permethylation of the cyclopentadienyl ligand and the influence of phosphane ligands with different π-accepting abilities. The ESR spectroscopic results reveal surprisingly large ^{31}P hyperfine coupling constants (hfcc). These can be explained by a superposition of two different electron spin transfer mechanisms, which include a σ- and a π-bonding mode between the Cr and Fe centers.

Keywords
bridging ligands · cyclooctatetraene · EPR spectroscopy · heterodinuclear complexes ·. structure elucidation

Introduction

In order to obtain a deeper insight into intermetallic communications in heterodinuclear complexes, we have examined the mutual influence of the metal centers in heterodinuclear complexes with a bridging cyclooctatetraene (Cot)[1, 2] which do not obey the 34 valence electron (VE) rule for dinuclear cycloolefinic-bridged complexes.[3, 4] In complexes with 34 VE two stable stereoisomers have been obtained, which show a synfacial (**A**) and an antifacial (**B**) coordination mode.[4–6]

Interestingly, both the antifacial and the synfacial complexes are diamagnetic, although a direct metal–metal bond can be excluded in the former because of the long metal–metal distance (> 370 pm). The strong electron–electron coupling between the metal centers must therefore occur through the bridging organic π ligand. Hence, it would be worthwhile to get more information about the interaction between both metal centers in antifacial μ-Cot complexes in comparison to corresponding synfacial derivatives. When compounds are paramagnetic, as in 33 VE complexes, ESR spectroscopy has been shown to be a very powerful tool for this purpose.[1, 2] There have not yet been any reports published on the successful synthesis of an antifacial complex with 33 VE. Since steric effects of the permethylated cyclopentadienyl ligand Cp* can force the formation of an antifacial configuration in some cases,[5] we employed $[CpCr(\eta^6\text{-Cot})]$ and $[Cp^*Cr(\eta^6\text{-Cot})]$[7] as the starting materials for synthesizing dinuclear paramagnetic 33 VE complexes of general

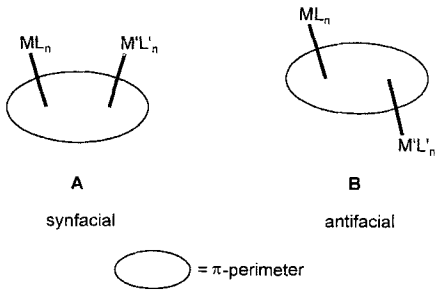

[*] Prof. Dr. J. Heck, Dr. G. Bögels, Dr. H. C. Brussaard, Dipl.-Chem. U. Hagenau, Prof. Dr. J. Kopf
Institut für Anorganische und Angewandte Chemie, Universität Hamburg
Martin-Luther-King-Platz 6, D-20146 Hamburg (Germany)
Fax: Int. code +(40)4123-6348
e-mail: heck@chemie.uni-hamburg.de
Dr. Ir. J. G. M. van der Linden, A. Roelofsen
Vakgroep Anorganische Chemie, Universiteit Nijmegen
Toenooiveld, NL-6525 ED Nijmegen (Netherlands)

[**] Cooperative effects in π ligand bridged dinuclear complexes, Part 21; Part 20: J. Heck, J. Körnich, *J. Organomet. Chem.* in press; Part 19: U. Hagenau, J. Heck, E. Hendrickx, A. Persoons, T. Schuld, H. Wong, *Inorg. Chem.* **1996**, *35*, 7863–7866.

  0947-6539/97/0307-1151 $ 17.50+.50/0

composition $[(C_5R_5)Cr(\mu\text{-Cot})Fe(CO)_3]$ (R = H: **1**; R = Me: **2**) with the aim of obtaining syn- as well as antifacially configurated products as a function of R. Additionally, we decided to exchange one CO ligand in **1** and **2** for phosphane ligands PR'_3 having different π-accepting abilities in order to control the metal–metal interaction. This interaction was investigated by X-ray structure determinations, electrochemistry, and ESR spectroscopy.

Results

Synthesis: The first synthesis of **1** was achieved through the reaction of $[(\eta^4\text{-Cot})Fe(CO)_3]$ with $[CpCrCl_2]$ under vigorous, reductive conditions.[2] However, with $[CpCr(\eta^6\text{-Cot})]$ and $[(CO)_3Fe(\eta\text{-}cis\text{-cyclooctene})_2]$[8] as starting materials, **1** was readily formed within a couple of hours under mild conditions and in high yields, owing to the lability of the *cis*-cyclooctene ligands in $[(CO)_3Fe(\eta\text{-}cis\text{-cyclooctene})_2]$ [Eq. (1), C_8H_{14} = *cis*-cyclooctene]. This type of reaction was also successful with the sterically demanding $[Cp^*Cr(\eta^6\text{-Cot})]$, which gave **2** in yields similar to those for **1**. The deep black-brown, air-sensitive products **1** and **2** contain 33 VE and are paramagnetic with one unpaired electron.

$$[(C_5R_5)Cr(\eta^6\text{-Cot})] + [(CO)_3Fe(\eta^2\text{-}C_8H_{14})_2] \longrightarrow [(C_5R_5)Cr(\mu\text{-Cot})Fe(CO)_3] + 2C_8H_{14} \quad (1)$$

1 (R = H), **2** (R = Me)

Abstract in German: *Die heterodinuclearen Komplexe $[(C_5R_5)Cr\{\mu\text{-}\eta^5(Cr):\eta^3(Fe)\text{-}Cot\}Fe(CO)_3]$ (R = H: **1**; R = Me: **2**; Cot = Cyclooctatetraen) werden in guten Ausbeuten durch die Reaktion von $[(C_5R_5)Cr(\eta^6\text{-Cot})]$ (R = H, Me) mit $[(CO)_3Fe(\eta\text{-cis-Cycloocten})_2]$ gebildet. In **1** und **2** läßt sich ein CO-Ligand leicht durch einen PR'_3-Liganden (R' = Me, Ph, OEt, F) substituieren, und man erhält $[(C_5R_5)Cr\{\mu\text{-}\eta^5(Cr):\eta^3(Fe)\text{-}Cot\}Fe(CO)_2PR'_3]$ (R = H, R' = Me: **3a**; R = H, R' = Ph: **3b**; R = Me, R' = Me: **4a**; R = Me, R' = Ph: **4b**; R = Me, R' = OEt: **4c**; R = Me, R' = F: **4d**). Die Ergebnisse von Einkristall-Röntgenstrukturuntersuchungen bestätigen ausschließlich die synfaciale Koordination der beiden Metall-Ligand-Fragmente in **2** und **4c** trotz des sperrigen C_5Me_5-(Cp*-) Liganden. Verglichen mit den C_5H_5-haltigen Produkten **1** und **3a** äußert sich der sterische Anspruch des Cp*-Liganden in **2** und **4c** durch zusätzliche Strukturverzerrungen und durch eine Verlängerung des Cr-Fe-Abstandes von 293 auf 303 bzw. 304 pm. Die heterodinuclearen Komplexe werden cyclovoltammetrisch und ESR-spektroskopisch untersucht, um den Einfluß der Permethylierung des Cyclopentadienylliganden sowie den Einfluß der Phosphanliganden mit unterschiedlichen π-Acceptoreigenschaften aufzuklären. Die ESR-spektroskopischen Ergebnisse zeigen überraschend große ^{31}P-Hyperfeinkopplungskonstanten. Sie lassen sich anhand zweier unabhängiger, sich ergänzender Elektronenspin-Übertragungsmechanismen erklären, denen sowohl ein σ- als auch π-Bindungsmodus zwischen den Cr- und Fe-Zentren zugrunde liegt.*

Complexes **1** and **2** reacted with phosphanes with substitution of one of the carbon monoxide ligands [Eq. (2), for substituents R and R', see Table 1].

$$[(C_5R_5)Cr(\mu\text{-Cot})Fe(CO)_3] + PR'_3 \longrightarrow [(C_5R_5)Cr(\mu\text{-Cot})Fe(CO)_2PR'_3] + CO \quad (2)$$

1, **2** → **3a,b**; **4a–d**

Table 1. Selected IR data for $[(C_5R_5)Cr(\mu\text{-Cot})Fe(CO)_2L]$.

	R	L	$\tilde{\nu}$(CO) [cm^{-1}]
1	H	CO	2003, 1930
3a	H	PMe_3	1932, 1881
3b	H	PPh_3	1936, 1886
2	Me	CO	1996, 1925
4a	Me	PMe_3	1924, 1872
4b	Me	PPh_3	1924, 1879
4c	Me	$P(OEt)_3$	1936, 1885
4d	Me	PF_3	1968, 1924

The reaction was monitored by IR spectroscopy. The starting compounds **1** and **2** show strong ν(CO) absorption bands at 2003 and 1930 cm^{-1} and 1996 and 1925 cm^{-1}, respectively, which are characteristic for a $M(CO)_3$ unit with local C_{3v} symmetry. These bands disappear, and two new ν(CO) bands of almost equal intensities appear at lower wavenumbers (Table 1). The yields of the desired phosphane-containing products were between 10 and 76%.

In the synthesis of **3a**, small amounts of volatile by-products were isolated in a cold-trap after the reaction mixture had been dried in vacuo. IR spectroscopic studies indicated the formation of $[Fe(CO)_5]$ and its PMe_3 derivatives $[Fe(CO)_{5-x}(PMe_3)_x]$ (x = 1, 2, 3).[9]

Structural Analyses: The X-ray structure analyses of **2**, **3a**, and **4c** (Figure 1, Table 2, and Table 7) revealed only synfacial configurations for the $(C_5R_5)Cr$ and $(CO)_2LFe$ (L = CO, PR'_3) units regardless of the nature of R (R = H, Me). The phosphorus-containing ligands in **3a** and **4c** are coordinated to the Fe center and are *trans* to the Cr atom. The Cot ligands are bound in an η^5 mode to the chromium center and η^3 to the iron center. This arrangement causes an interruption in the conjugation of the Cot carbon atoms, as shown by the distinct elongation of the C(3)–C(4) and C(6)–C(7) bond lengths (Table 2). The $Cr\text{–}C_{Cot}$ bond lengths are similar to those observed for (η^5-pentadienyl)chromium fragments,[10] and the $Fe\text{–}C_{Cot}$ distances show the same long–short–long alternation as that seen in $[\{(\eta^3\text{-}C_3H_5)Fe(CO)_3\}_2]$[11] and other heterodinuclear Fe complexes that contain an $\eta^3(Fe)$-allylic bonding mode of the olefinic ligand.[12] The Cr–Fe distance is 292.83(8) pm for the Cp derivative **3a**, which is almost identical to the Cr–Fe distance in **1**,[2] and about 10 pm longer for the Cp* compounds **2** and **4c** as a result of the steric demand of the Cp* ligand. These metal–metal distances represent a long Cr–Fe single bond, when compared to those found in other Cr/Fe species[13] and to the hypothetical Cr–Fe single-bond length of 320 pm, estimated from the metal–metal distances in $[\{CpCr(CO)_3\}_2]$[14] and $[\{(\eta^3\text{-allyl})Fe(CO)_3\}_2]$.[11]

0947-6539/97/0307-1152 $ 17.50+.50/0 Chem. Eur. J. 1997, 3, No. 7

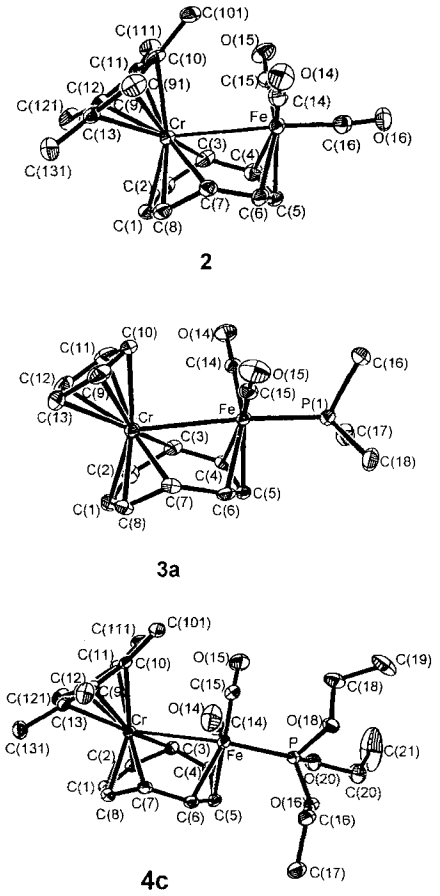

Figure 1. ORTEP drawings of the molecular structure of **2**, **3a**, and **4c** (the hydrogen atoms are omitted for clarity, ellipsoids at the 50% probability level).

The steric demand of the bulky Cp* ligand is also indicated by several other structural features:

1) The Cr–C(10) bond in **2** and **4c** is about 6–8 pm longer than the shortest bond between the Cr center and the cyclopentadienyl ligand, while the corresponding difference in Cp derivatives such as **1** and **3a** is about 3.5 pm.
2) The Me group C(101) is deflected by about 10° from the cyclo-C_5 plane of Cp* (Figure 1).
3) The cyclopentadienyl plane and η^5-Cot plane show a larger deviation from parallelism in **2** and **4c** than in **3a** (Table 2).

The substitution of one CO by a phosphorus-containing ligand only influences the Cr–Fe distance slightly, if at all (see complex **2** and **4c**), and results in a small Fe–C(14) and Fe–C(15) bond shortening and a corresponding C(14)–O(14) and C(15)–O(15) bond elongation due to increased π back donation from the Fe center to the remaining CO ligands. This is also confirmed by the low-energy shift of the CO stretching vibration in **3a**,**b** and **4a**–**d** relative to those of **1** and **2** (Table 1).

ESR Spectroscopy: All of the heterodinuclear compounds presented here show highly resolved solution ESR spectra with hyperfine structure (hfs) from ^1H and ^{53}Cr as well as hfs from ^{31}P in **3a**,**b** and **4a**–**d** (Figure 2). The hf coupling constants (hfcc) (Table 3) were determined by calculations of the experimental spectra. The g_{iso} values obtained in this way as well as ^1H and ^{53}Cr hfcc strongly resemble those of the mononuclear com-

Table 2. Selected bond lengths [pm] and angles [°] of $[(C_5R_5)Cr\{\mu\text{-}\eta^5(Cr):\eta^3(Fe)\text{-Cot}\}Fe(CO)_2L]$ (R = Me, L = CO: **2**; R = H, L = PMe_3: **3a**; R = Me, L = $P(OEt)_3$: **4c**).

	2	**3a**	**4c**
Fe–Cr [a]	303.31(8)	292.83(8)	304.52(5)
Cr–C(1)	217.2(4)	215.1(3)	216.5(3)
Cr–C(2)	212.9(4)	212.1(3)	213.2(3)
Cr–C(3)	217.5(4)	215.9(3)	217.3(3)
Cr–C(7)	217.8(4)	214.5(3)	218.4(3)
Cr–C(8)	213.6(4)	211.2(3)	212.2(3)
Cr–C(9)	222.5(4)	219.8(3)	223.7(3)
Cr–C(10)	228.0(4)	221.7(3)	228.5(3)
Cr–C(11)	224.5(4)	219.9(4)	224.1(3)
Cr–C(12)	221.6(4)	218.2(4)	220.0(3)
Cr–C(13)	221.8(4)	218.7(4)	220.1(3)
Fe–C(4)	214.3(4)	210.3(3)	213.4(3)
Fe–C(5)	206.8(4)	205.9(3)	206.6(3)
Fe–C(6)	214.4(4)	212.5(3)	212.7(3)
Fe–C(14)	179.9(5)	176.2(3)	177.6(4)
Fe–C(15)	180.1(5)	176.7(3)	177.0(4)
Fe–L [b]	180.9(5)	221.6(2)	217.4(1)
C(1)–C(2)	141.1(7)	142.0(5)	142.0(5
C(2)–C(3)	142.3(7)	142.5(5)	143.4(5)
C(3)–C(4)	146.8(6)	146.1(5)	147.3(5)
C(4)–C(5)	142.2(6)	140.0(5)	141.1(5)
C(5)–C(6)	140.0(7)	140.8(5)	141.3(5)
C(6)–C(7)	146.9(6)	145.5(5)	146.5(4)
C(7)–C(8)	143.4(6)	142.7(5)	143.4(4)
C(8)–C(1)	140.9(6)	140.7(5)	141.5(3)
C(14)–O(14)	114.4(6)	116.3(4)	115.9(4)
C(15)–O(15)	114.1(6)	114.7(4)	116.2(4)
C(16)–O(16)	114.9(6)		
Cr-Fe-L [b]	175	173	170
$[\eta^5(Cr):\eta^3(Fe)\text{-Cot}]$ [c]	50.44	49.62	51.19
$[C_5R_5\text{-}\eta^5(Cr)\text{-Cot}]$ [d]	9.16	3.92	10.41
C(101)–C_5Me_5 [e]	11.99		12.36
C(14)-Fe-L [b]	95.0(2)	95.2(1)	96.3(1)
C(14)-Fe-C(15)	104.1(2)	100.9(2)	103.0(2)
C(15)-Fe-L [b]	94.0(2)	92.7(1)	94.7(1)
Fe-C(14)-O(14)	175.2(4)	179.9(3)	177.4(3)
Fe-C(15)-O(15)	175.0(4)	177.9(3)	177.0(3)

[a] Cr–Fe distance in **1**: 293.69(13) pm [2]. [b] L represents the *ipso* atom linked to Fe, i.e., C or P. [c] Angle between the best planes of the $\eta^5(Cr)$ and $\eta^3(Fe)$ unit of the Cot ligand, e.g., 50.4° for **1** [2]. [d] Angle between the best planes of the C_5R_5 ligand and $\eta^5(Cr)$ unit of the Cot ligand. [e] Angle between the bond vector C(19)–C(101) and the best plane of the C_5Me_5 ligand.

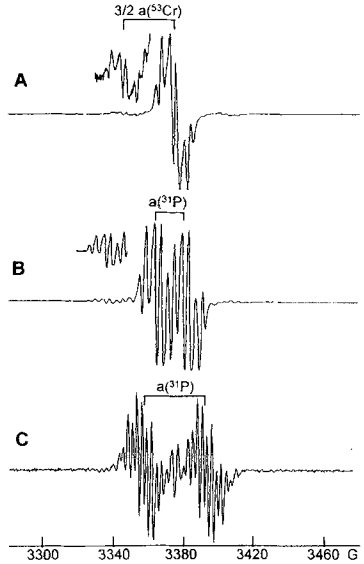

Figure 2. Solution ESR spectra of **2** (A), **4b** (B), and **4d** (C) (MTHF, 293 K, X-band).

Table 3. ESR data of $[(C_5R_5)Cr\{\mu\text{-}\eta^5(Cr):\eta^3(Fe)\text{-}Cot\}Fe(CO)_2L]$.

	R	L	g_{iso} [a]	$g_\perp$ [b]	$g_\parallel$ [b]	$a(^{53}Cr)$ [c]	$a(^{31}P)$[d]	$a(^1H)$ [d]	$A_\perp(^{31}P)$ [e]	$A_\parallel(^{31}P)$ [e]
1	H	CO [2]	1.991	1.982	2.008	19.0	–	5.04 (2,8-H) 3.32 (3,7-H) 3.32 (1-H)	–	–
3a	H	PMe_3	1.995	1.990	2.010	19.0	13.3	5.4 (2,8-H) 3.2 (3,7-H) 3.7 (1-H)	12.0	15.0
3b	H	PPh_3	1.9925	1.986	2.008	19.0	13.6	5.1 (2,8-H) 3.1 (3,7-H) 3.9 (1-H)	13.0	13.0
2	Me	CO	1.9939	1.986	2.008	18.9	–	4.8 (2,8-H) 3.3 (3,7-H) 2.55 (1-H)		
4a	Me	PMe_3	1.9931	1.986	2.008	18.9	15.3	4.8 (2,8-H) 3.1 (3,7-H) 3.6 (1-H)	15.0	14.0
4b	Me	PPh_3	1.9927	1.986	2.009	19.0	15.3	4.8 (2,8-H) 3.1 (3,7-H) 3.6 (1-H)	14.7	14.3
4c	Me	$P(OEt)_3$	1.9931	1.986	2.007	19.0	23.5	4.8 (2,8-H) 3.2 (3,7-H) 3.4 (1-H)	23.0	21.0
4d [f]	Me	PF_3	1.9942	1.987	2.011	18.5	34.2	4.8 (2,8 H) 3.5 (3,7-H) 2.5 (1-H)	33.5	31.5

[a] $\pm < 0.001$ for **1**, **3a**; $\pm < 0.0005$ for **2**, **3b**, **4a**–**4d**. [b] $\pm < 0.002$. [c] In Gauss, $\pm < 0.5$. [d] In Gauss, $\pm < 0.1$ except for **1**. [e] In Gauss, $\pm < 0.2$. [f] $a(^{19}F) = 5.5(1)$ G.

plexes $[CpCr(\eta^6\text{-Cot})]$ and $[Cp^*Cr(\eta^6\text{-Cot})]$.[7] These results justify the assumption that the unpaired electron is predominantly localized in a d_{z^2}-type orbital at the Cr center. When a direct spin delocalization from the semi-occupied d_{z^2}-type orbital of the Cr center into the C–H σ bond is taken into account,[15a] the value of the ^1H hfcc is found to depend on the distance between the metal and the corresponding carbon atom.[15b] Therefore the assignments of the ^1H hfcc in Table 3 are based on structural arguments. In comparison to the mononuclear complexes, the ^1H hfs of the dinuclear species is reduced by one ^1H hfcc with $a(1\,^1H) > 3$ G, which is in accordance with the change in the hapticity with which the Cot ligand coordinates to the Cr center on going from the mononuclear $\eta^6(Cr)$ to the dinuclear $\eta^5(Cr)$ bonding mode. The isotopic g values of the dinuclear complexes show a slight increase for **1**–**4d** compared to the mononuclear compounds $[(C_5R_5)Cr(\eta^6\text{-Cot})]$ (R = H, Me), indicating the subtle influence of the heavier atoms Fe and P.

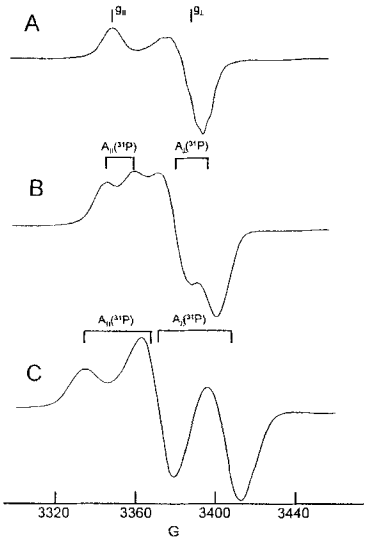

Figure 3. Solid-solution ESR spectra of **2** (A), **4b** (B), and **4d** (C) (MTHF, 120 K, X-band).

The solid-solution EPR spectra of **1**–**4d** only show two g values close to 2.0 (Figure 3, Table 3), representing an axial g tensor. Whereas a fairly good resolution for the ^{31}P hfs can be observed on $g_\parallel$ and on $g_\perp$ for **3a,b** and **4a**–**d**, the ^1H hfs remains unresolved in all cases. This unresolved ^1H hfs makes considerable contributions to the line width, preventing an accurate determination of $g_\parallel$ and $g_\perp$ as well as $A_\parallel(^{31}P)$ and $A_\perp(^{31}P)$ by the calculation of the experimental spectra. The latter would have been worthwhile for calculating the anisotropic part of the ^{31}P hfc, from which the π-electron density on the phosphorus atom could have been estimated.[16] However, $A_\parallel(^{31}P)$ and $A_\perp(^{31}P)$ only differ to a small extent and are nearly as large as $a_{iso}(^{31}P)$, indicating the same sign of $A_\parallel$, $A_\perp$, and a_{iso}.

Redox Chemistry: The cyclic voltammograms (CV) of the complexes **1** and **2** (Figure 4A) show one electrochemically reversible redox couple (0/+1) at

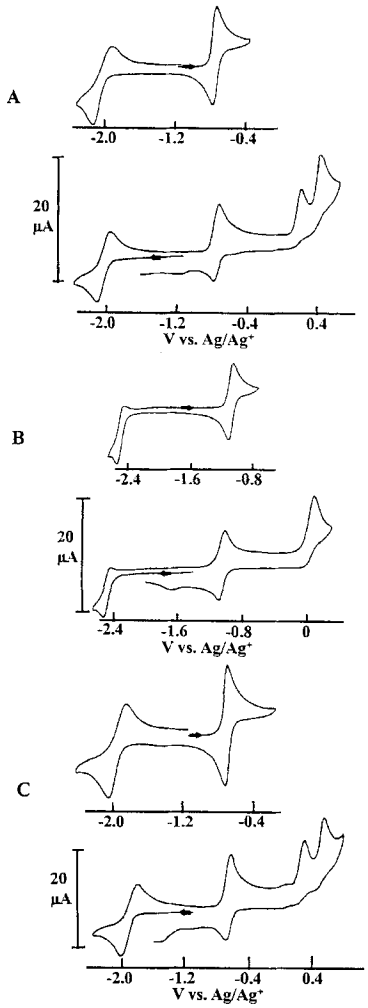

Figure 4. Cyclic voltammograms of **2** (A), **3a** (B), and **4d** (C) (for more details, see text and experimental section).

0947-6539/97/0307-1154 $ 17.50+.50/0 Chem. Eur. J. 1997, 3, No. 7

Table 4. Cyclic voltammetry data [a] of $[(C_5R_5)Cr\{\mu\text{-}\eta^5(Cr):\eta^3(Fe)\text{-}Cot\}Fe(CO)_2L]$.

	R	L	E_{eq} [b]	$E_{1/2}$ [b] (0/−1)	ΔE_p [b]	i_{pc}/i_{pa}	$E_{1/2}$ [b] (0/+1)	ΔE_p [b]	i_{pc}/i_{pa}	E_{pa} [b] (+1/+2)	E_{pa} [b] (+2/+3)
1	H	CO	−0.75	−2.03	80	1	−0.64	65	1	0.38	0.47
3a	H	PMe_3	−1.16	−2.53 [c]	130	<1	−1.08	61	1	0.05 [f]	
3b	H	PPh_3	−0.92	−2.43 [d,e]	–	–	−0.90	68	1	0.15 [f]	
2	Me	CO	−0.85	−2.03 [c]	200	≈1	−0.74	77	1	0.23	0.46
4a	Me	PMe_3	−1.30	−2.52 [c]	110	<1	−1.19	59	1	−0.03 [f]	
4b	Me	PPh_3	−1.10	−2.48 [d,e]	–		−1.01	59	1	0.02 [g]	0.10 [g]
4c	Me	$P(OEt)_3$	−1.17	−2.38 [c]	160	<1	−1.07	62	1	−0.03 [g]	0.07 [g]
4d	Me	PF_3	−0.85	−1.94 [c]	210	<1	−0.67	62	1	0.29	0.51

[a] DME, 0.1 M $TBAPF_6$, Pt working electrode, Ag/Ag^+ with 0.1 M Ag triflate as the reference electrode. [b] E_{eq} (equilibrium potential), $E_{1/2}$, E_{pc}, E_{pa} in Volts vs. FcH/FcH^+ (FcH = ferrocene), ΔE_p in mV. [c] ΔE_p depends on the scan rate v, but $E_{1/2} = 1/2(E_{pc} + E_{pa})$ remains constant. [d] Only peak potential E_{pc} is given. [e] Peak current decreases with increasing scan rate. [f] Irreversible two-electron oxidation (+1/+3). [g] Poorly resolved.

−0.64 and −0.74 V vs. FcH/FcH^+ (FcH = ferrocene), respectively, and two completely irreversible oxidation steps beyond 0 V.

A reduction wave (0/−1) occurs at −2 V for **1** and **2**. For **1** this is electrochemically reversible (Table 4), whereas for **2** the difference in the peak potentials ΔE_p of the redox couple 0/−1 depends on the scan rate v; this indicates a chemically reversible reaction upon uptake of an electron. An additional couple −1/−2 for **1** and **2** (not depicted) is at the potential limit of the solvent, preventing an exact determination of the ratio of the peak currents. Nevertheless, the observed independence of the peak potentials from the scan rate v indicates electrochemical reversibility of the redox couple −1/−2.

The features in the CV of the phosphane-containing complexes **3a,b** and **4a–d** (Figure 4B,C) resemble those of **1** and **2**. A completely irreversible oxidation step is found at about 0 V, which seems to be a two-electron transfer step for **3a**, **3b**, and **4a**; for **4b–d** (Figure 4C), these irreversible oxidations are resolved as two one-electron transfers. An electrochemically reversible oxidation is located near −1 V, with the exception of **4d** whose corresponding oxidation potential is shifted to −0.62 V. For **4a–c** a reduction step (0/−1) can be recorded clearly below −2 V, near the potential limit of the solvent, while for **4d** the first reduction occurs slightly above −2 V. However, the peak potentials depend on the scan rate; this shows that the redox couple 0/−1 is at least electrochemically irreversible. In cases where a reoxidation wave can be observed (e.g. **4a**, **4c**, **4d**), $E_{1/2} = 1/2(E_{pc} + E_{pa})$ remains constant.

A comparison of the redox potentials of **1–4c** shows that a distinct cathodic shift of more than 250 mV can generally be observed on going from **1** and **2** with $Fe(CO)_3$ fragments to the corresponding phosphane-containing species. The redox waves for **4d** display an anodic shift with respect to the corresponding potentials of **2**, reflecting the strong π-acidity of PF_3. The change from Cp to Cp* only causes a cathodic shift of about 100 mV for the first reversible oxidation step and of only 40–50 mV for the first reduction step.

Discussion

The heterodinuclear complexes of composition $[(C_5R_5)Cr(\mu\text{-}Cot)Fe(CO)_3]$ (**1**, R = H; **2**, R = Me) were obtained in comparably good yields from the reaction of $[(CO_3)Fe(cis\text{-}cyclooctene)_2]$ with $[CpCr(\eta^6\text{-}Cot)]$ and $[Cp^*Cr(\eta^6\text{-}Cot)]$, respectively. In spite of the bulkier Cp* ligand in **2**, both complexes have the same synfacial configuration. No indication was found for the formation of an antifacial derivative in the case of Cp*, although it contains only one electron less than the 34 VE species, which allow both configurations. The formation of exclusively synfacial products may have two different causes:

1) The steric interactions with the permethylated cyclopentadienyl ligand in the synfacial configuration, which have been shown to give rise to distortions in the crystal structure, are not sufficient to overcome the reduction in stability on formation of antifacial species with less than 34 VE.
2) The free double bond in the starting materials $[CpCr(\eta^6\text{-}Cot)]$ and $[Cp^*Cr(\eta^6\text{-}Cot)]$ is only accessible for coordination from the *endo* face with respect to the chromium center (Scheme 1), since the free double bond is bent away from the plane of the six metal-bound carbon atoms by about 64°.[17]

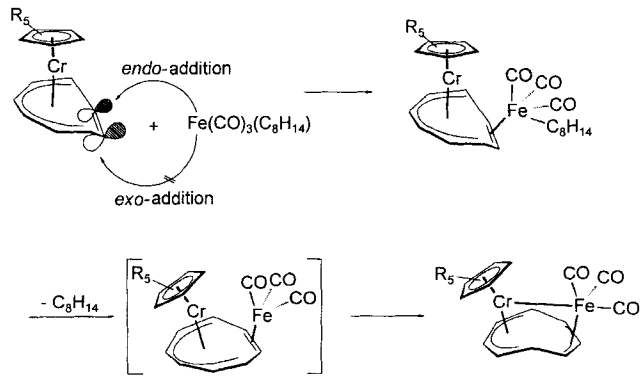

Scheme 1. Suggested reaction pathway of the formation of **1** and **2** (R = H, Me).

A remarkable feature of the Cp* complex **2** is the faster substitution of CO by phosphanes compared to the Cp derivative **1**, although one would expect a larger steric hindrance of the Cp* ligand. The acceleration of the CO substitution in **2** may be due to a weakening of the Cr–Fe bond, reflected by the elongation of about 10 pm, which facilitates the homolysis of the metal–metal bond. The product of the homolysis would contain a 16 VE unit $[Cp^*Cr(\eta^5\text{-}Cot)]$ and a 17 VE unit $[(CO)_3Fe(\eta^3\text{-}Cot)]$ (Scheme 2a). The 17 VE allyl complex $[(CO)_3Fe(\eta^3\text{-}C_3H_5)]$ also readily undergoes CO substitution reactions with phosphanes,[8,9] believed to involve an intermediate or transition state with 19 VE.[9] Subsequent elimination of CO yields

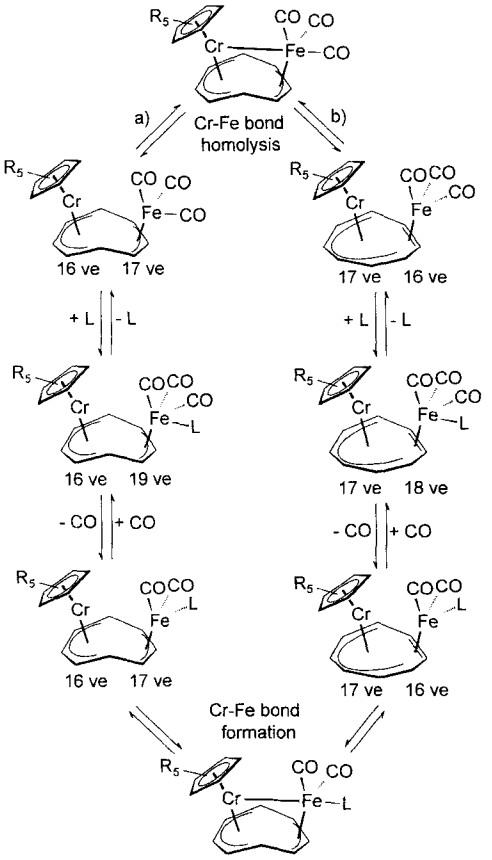

Scheme 2. Suggested reaction pathways of the CO substitution reactions (R = H, Me).

the product. An alternative route includes a change of the hapticity of the Cot ligand after Cr–Fe bond homolysis occurs—a reversal of the formation of **1** and **2** (Scheme 2b; cf. Scheme 1).

The 16 VE fragment $[(CO)_3Fe(\eta^2\text{-Cot})]$ readily coordinates to a phosphane ligand, and the products are subsequently formed by elimination of one CO. In addition, the 17 VE allylic as well as the 16 VE olefinic $[Fe(CO)_2PR'_3]$ species can rotate around the η^3- or η^2-carbon–metal bond, respectively, which enables the sterically more demanding PR'_3 ligand to adopt a *trans* arrangement. In competition to the CO elimination, the bond between the Cot ligand and $[Fe(CO)_3PR'_3]$ may be cleaved yielding an unsaturated mononuclear species, which rapidly adds CO or PR'_3 from the reaction solution. The observed formation of $[Fe(CO)_{5-x}L_x]$ ($L = PMe_3$) in the reaction of **1** with PMe_3 confirms this possible side reaction.

In contrast to the influence of the Cp* ligand on the Cr–Fe bond lengths, the change of the ligands L *trans* to the chromium center, for example, from **1** (L = CO) to **3a** ($L = PMe_3$) and from **2** (L = CO) to **4c** ($L = P(OEt)_3$), does not alter the Cr–Fe bond length significantly. This is surprising given the fact that a strong π acceptor (CO) is substituted by a medium π acceptor (PMe_3, $P(OEt)_3$) and that the Cr-Fe-L unit is in an almost linear arrangement and is thus set up for a *trans* effect.

Although weak, the chromium–iron bonds in the dinuclear compounds under investigation are confirmed to exist by ESR spectroscopy. The most striking differences within the ESR spectra of all of the dinuclear compounds is the unexpectedly large ^{31}P hfcc of **3a–4d**, which roughly doubles the isotropic hfs of **1** and **2**. The ^{31}P hfcc are similar to ^{31}P hfcc of 17 VE half-sandwich compounds with PR'_3 ligands directly linked to the paramagnetic center,[20] although the phosphane ligands in **3a, b** and **4a–d** are coordinated to the iron centers and not to the paramagnetic Cr centers, as shown by X-ray structure analyses. Hence, a very effective electron spin transfer must occur from the Cr center to the P atom.

Presumably, the electron spin is transferred in two different ways (Figure 5). Firstly, the unpaired Cr d_{z^2}-type electron induces a spin polarization of the electron pair of the Cr–Fe σ bond, which causes a corresponding spin polarization of the Fe–P bonding electrons. This polarization manifests itself in an excess of positive spin density at the ^{31}P nucleus (Figure 5A). Secondly, an electron spin delocalization may occur through orbitals of π-bonding character (Figure 5B). The Cr-Fe-P

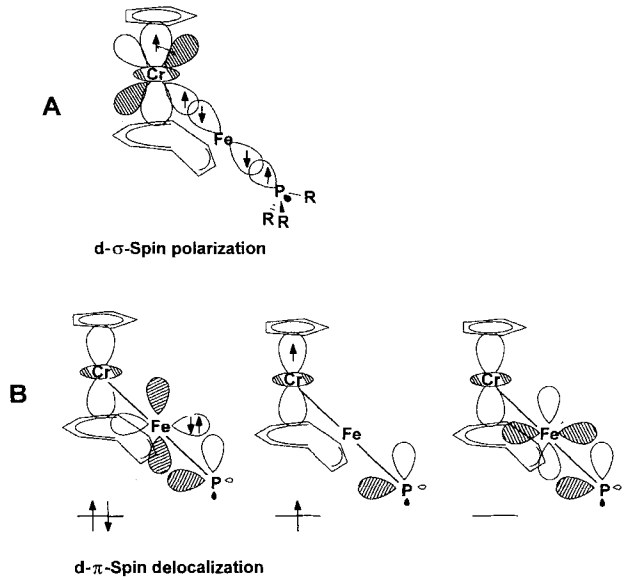

Figure 5. Possible pathways of spin transfer from the Cr center to the P atom: A) spin σ polarization; B) spin π delocalization.

grouping may be regarded as a 3-center/3 π-electron system with an interaction between the Cr–d_{z^2} orbital, a d-type orbital of the iron center, and a suitable σ* orbital of the P ligand,[21] leading to a doubly occupied bonding, a semi-occupied nonbonding, and an empty antibonding molecular orbital. Consequently, this type of π delocalization yields a population of positive electron spin density at the phosphorus atom, similar to that induced by the σ-spin polarization. The importance of the π-delocalization mechanism for the ^{31}P hfcc is recognized from the distinct increase of the ^{31}P hfcc with increasing π-acidity of the phosphorus-containing ligands.[22] The increased π-acidity is also reflected in the energy of the CO stretching vibrations (Table 1), in the change of the redox potentials (Table 4), and in the slight shortening of the Fe–L bond in **4c** as compared to **3a** (Table 2).

A spin transfer through the bridging Cot ligand may be excluded from consideration. The spin transfer between the Cr and Fe center would then have to occur through the carbon–carbon single bonds between C(3)–C(4) and C(6)–C(7), which normally lowers the spin density by an order of magnitude.

0947-6539/97/0307-1156 $ 17.50+.50/0 Chem. Eur. J. 1997, 3, No. 7

A low spin density in the distal part of a cyclo-C_8 ligand, which is not coordinated to the paramagnetic center of mononuclear d^5 complexes such as [CpCr(η^6-Cot)][7] and [CpV(η^7-C_8H_9)],[23] is indicated by $a(^1H)$ hfcc of about 1 G or smaller for protons in the β-position.

In addition to the increase of the ^{31}P hfcc from **4a** to **4d**, there is a decrease of the ^1H hfcc of 1-H, which sits opposite the PR'_3 ligand. Interestingly, the change of the ^1H hfcc of 1-H is accompanied by small, but noticeable structural changes: lengthening of the bond between Cr and C(1) can be observed with the decrease of the ^1H hfcc of 1-H (Table 5). Apparently, an increase of the π-acidity of the phosphane ligand weakens the *trans*-positioned Cr–C(1) bond. This special "long range" *trans* effect can only occur through a direct Cr–Fe bond, although it is presumably a weak one.

Table 5. Selected structural and ESR spectroscopic data to indicate a "long range" *trans*-effect in $[(C_5R_5)Cr\{\mu\text{-}\eta^5(Cr):\eta^3(Fe)\text{-Cot}\}Fe(CO)_2L]$.

	R	L	$a(1\,^1H)$ [G]	$a(^{31}P)$ [G]	d(Cr–C(1)) [pm]
2	Me	CO	2.6	–	217.2(4)
4c	Me	$P(OEt)_3$	3.4	23.5	216.5(3)
3a	*H*	PMe_3	3.7	13.3	215.1(3)

The assumption of a Cr–Fe bond does not contradict the axial g tensor found for **1**–**4d**. As already outlined, the ESR data point to a d_{z^2}-type SOMO, which is known to be almost nonbonding with respect to the π ligand. Hence, changes in symmetry of the π ligand or changes in the nature of the coordinating atoms lying in plane with the π ligand only cause small perturbations in the symmetry of the SOMO.[7, 24a]

The population of a SOMO with a predominant Cr–d_{z^2} character in the heterodinuclear complexes **1**–**4d** also agrees with the results of the CV measurements. The induced cathodic shift of 20 mV and less per methyl group, on changing from the compounds with unmethylated Cp (**1**, **3a**, **3b**) to the corresponding Cp* derivatives (e.g., for the oxidation step $0/+1$ and the reduction step $0/-1$), is characteristic for sandwich-type complexes containing a SOMO with a d_{z^2}-type orbital that is almost nonbonding with respect to the aromatic ligand.[24b, 25]

In contrast, the substitution of one CO by PR'_3 causes shifts in the redox potentials ranging from a 500 mV cathodic shift to a 90 mV anodic shift with respect to the potentials of the corresponding CO compounds **1** and **2**, depending on the π-acidity of PR'_3; all of the redox couples are distinctly influenced by the nature of the PR'_3 ligand. This observation is in accordance with the outlined σ and π interactions explaining the unexpectedly large ^{31}P hfcc obtained from ESR spectra.

Finally, it is of interest to compare the redox properties of the synfacial 33 VE complexes with those of the 34 VE antifacial complexes. The latter only show two-electron oxidations at ambient temperatures;[26] this is accompanied by a Cot ring cleavage, after which the formation of a metal–metal bond is possible. Apparently, an antifacial configuration with 33 VE is not sufficiently stable to be recognized—at least for homodinuclear complexes—even on the electrochemical timescale.

Summary

The reaction of $[(C_5R_5)Cr(\eta^6\text{-Cot})]$ (R = H, Me) with $[(CO)_3Fe(\eta\text{-}cis\text{-cyclooctene})_2]$ yields the heterodinuclear μ-Cot complexes $[(C_5R_5)Cr\{(\mu\text{-}\eta^5(Cr)\text{: }\eta^3(Fe)\text{-Cot}\}Fe(CO)_3]$ exclusively with a synfacial coordination mode, regardless of the nature of R. These complexes undergo facile thermal substitution reactions of one CO by PR'_3 (R = Me, Ph, OEt, F) to produce $[(C_5R_5)Cr\{(\mu\text{-}\eta^5(Cr):\eta^3(Fe)\text{-Cot}\}Fe(CO)_2PR'_3]$. X-ray structure analyses indicate the presence of a long Cr–Fe single bond, which stretches by about 10 pm when the Cp ligand is replaced by the sterically demanding Cp* ligand. ESR spectroscopic studies reveal surprisingly high ^{31}P hfcc. These are explained by two different spin transfer mechanisms based on σ- and π-bonding interactions of the trinuclear Cr-Fe-P group and confirm the presence of a direct Cr–Fe bond. These bonding interactions also explain the dependence of the redox potentials on the π-accepting ability of the *trans* ligand at the Fe center.

Experimental Section

All manipulations were carried out under an N_2 atmosphere and in solvents saturated with N_2. Tetrahydrofuran (THF) and 2-methyltetrahydrofuran (MTHF) were freshly distilled from potassium metal/benzophenone; *n*-hexane was distilled from K/Na alloy, toluene from Na. IR: THF solutions were measured against pure THF, when not otherwise stated, KBr cells, FT-IR 1720X (Perkin Elmer). Cyclic voltammetry: DME, 0.1 M $(n\text{Bu})_4NPF_6$ ($TBAPF_6$), Pt working electrode (disk, ∅ 3 mm), Pt wire as an auxilliary electrode, Ag/0.1 M silver triflate as a reference electrode, PAR 273 potentiostat (E & EG). ESR: MTHF solutions, ESP 300 (Bruker); the recorded spectra were simulated with the software program simphonia (Bruker). EI-MS: 70 eV, Finnigan MAT 311 A. Elemental analysis: Heraeus CHN-O-Rapid, Institut für Anorganische und Angewandte Chemie, Universität Hamburg. $[CpCr(\eta^6\text{-Cot})]$,[7] $[Cp^*Cr(\eta^6\text{-Cot})]$[7] and $[(CO)_3Fe(\eta\text{-}cis\text{-cyclooctene})_2]$[8] were synthesized according to the literature. PF_3 was kindly donated by Prof. Kruck, Institut für Anorganische Chemie, Universität Köln.

$[(C_5H_5)Cr\{\mu\text{-}\eta^5(Cr):\eta^3(Fe)\text{-Cot}\}Fe(CO)_3]$ (1): A mixture of $[CpCr(\eta^6\text{-Cot})]$ (0.86 g, 3.11 mmol) and $[(CO)_3Fe(\eta\text{-}cis\text{-cyclooctene})]$ (1.12 g, 3.11 mmol) in pentane was stirred for 2 h at −78 °C. The reaction mixture was allowed to warm to room temperature and filtered through a short plug of celite. The solvent was concentrated until crystallization started. After storage at −30 °C for 2 d, 0.91 g (81%) of **1** was obtained.

$[(C_5Me_5)Cr\{\mu\text{-}\eta^5(Cr):\eta^3(Fe)\text{-Cot}\}Fe(CO)_3]$ (2): The synthesis was performed as for **1**. $[Cp^*Cr(\eta^6\text{-Cot})]$ (2.04 g, 7.0 mmol) and $[(CO)_3Fe(cis\text{-cyclooctene})_2]$ (2.17 g, 7.0 mmol) were reacted at −78 °C for 3 h to yield 2.56 g (85%) of **2**. M.p. 139 °C (in closed capillary); IR (nujol): $\tilde{\nu}$ = 2002, 1931 cm^{-1}; EI-MS: m/z (%) = 431 (0.01) $[M^+]$, 403 (16) $[M^+ - CO]$, 375 (17) $[M^+ - 2CO]$, 347 (100) $[M^+ - 3CO]$, 319 (36), 291 (78) $[(Cp^*CrCot)^+]$, 276 (21), 251 (11), 187 (88) $[(Cp^*Cr)^+]$, 133 (21), 91 (3) $[(C_7H_7)^+]$, 52 (47) $[Cr^+]$; $C_{21}H_{23}CrFeO_3$ (427.3); calcd C 58.49, H 5.38; found C 58.53, H 5.26.

$[(C_5R_5)Cr\{\mu\text{-}\eta^5(Cr):\eta^3(Fe)\text{-Cot}\}Fe(CO)_2PR'_3]$ (3a–4c): In a typical reaction an equimolar amount of PR'_3 and **1** or **2** were stirred at room temperature. The scope of the reaction was monitored by IR spectroscopy. During the reaction additional PR'_3 (R' = Me, Ph) was added periodically until the ν(CO) bands of the starting material had disappeared. The solvent was removed in vacuo and the residue was extracted with *n*-hexane. The hexane extract was filtered through celite and reduced until a crystalline material precipitated. After storage of this solution at −30 °C for 2 d, the product was obtained as a brownish black crystalline material. It is very sensitive to oxygen in solution. See Table 6 for quantities used, reaction time and yields.

Table 6. Conditions [a] for the CO substitution reaction in **1** and **2** with PR'_3.

SM	g(mmol)	PR'_3	g(mmol)	Prod.	t	Yield
1	1.08 (2.99)	PMe_3	0.68 (9.0)	**3a**	7 d	42
	0.48 (1.11)	PPh_3	0.68 (2.59)	**3b**	7 d	45
2	0.97 (2.23)	PMe_3	0.51 (6.7)	**4a**	3 d	76
	0.80 (1.85)	PPh_3	1.29 (4.92)	**4b**	3 d	54
	0.89 (2.06)	$P(OEt)_3$	0.34 (2.04)	**4c**	27 h	61
	0.61 (1.42)	PF_3	[b]	**4d**	3 h	10

[a] The reactions were performed at room temperature. [b] PF_3 gas was bubbled through the reaction mixture; for further details see the experimental section.

$[(C_5H_5)Cr\{\mu\text{-}\eta^5(Cr)\text{:}\eta^3(Fe)\text{-Cot}\}Fe(CO)_2PMe_3]$ (3a): EI-MS: m/z (%): 409 (2) $[M^+]$, 353 (5) $[M^+ - 2CO]$, 333 (2) $[M^+ - PMe_3]$, 305 (4) $[M^+ - PMe_3 - CO]$, 277 (37) $[M^+ - PMe_3 - 2CO]$, 221 (32) $[(CpCrCot)^+]$, 195 (12) $[(CpCrC_6H_6)^+]$, 117 (94) $[(CpCr)^+]$, 104 (100) $[Cot^+]$, 76 (63) $[(PMe_3)^+]$, 61 (94) $[(PMe_2)^+]$, 52 (38) $[Cr^+]$; $C_{18}H_{22}CrFeO_2P$ (409.22); calcd C 52.83, H 5.43; found C 52.45, H 5.52.

$[(C_5H_5)Cr\{\mu\text{-}\eta^5(Cr)\text{:}\eta^3(Fe)\text{-Cot}\}Fe(CO)_2PPh_3]$ (3b): EI-MS: m/z (%) = 595 (0.01) $[M^+]$, 333 (1) $[M^+ - PPh_3]$, 305 (2) $[M^+ - PPh_3 - CO]$, 277 (9) $[M^+ - PPh_3 - 2CO]$, 262 (100) $[(PPh_3)^+]$, 221 (13) $[CpCrCot^+]$, 185 (70) $[(PPh_2)^+]$, 117 (42) $[(CpCr)^+]$, 108 (33) $[(PPh)^+]$, 104 (11) $[Cot^+]$, 77 (13) $[Ph^+]$, 65 (7) $[Cp^+]$, 52 (34) $[Cr^+]$; $C_{33}H_{28}CrFeO_2P$ (479.33); calcd C 66.57, H 4.75; found C 66.20, H 4.93.

$[(C_5Me_5)Cr\{\mu\text{-}\eta^5(Cr)\text{:}\eta^3(Fe)\text{-Cot}\}Fe(CO)_2PMe_3]$ (4a): EI-MS: m/z (%): 479 (0,4) $[M^+]$, 403 (3) $[M^+ - PMe_3]$, 375 (3) $[M^+ - PMe_3 - CO]$, 347 (20) $[M^+ - PMe_3 - 2CO]$, 291 (32) $[(Cp^*CrCot)^+]$, 187 (59) $[(Cp^*Cr)^+]$, 133 (20), 76 (28) $[(PMe_3)^+]$, 61 (43) $[(PMe_2)^+]$, 52 (100) $[Cr^+]$, 46 (4) $[(PMe^+)]$; $C_{23}H_{32}CrFeO_2P$ (479.33); calcd C 57.63, H 6.73; found C 57.20, H 6.70.

$[(C_5Me_5)Cr\{\mu\text{-}\eta^5(Cr)\text{:}\eta^3(Fe)\text{-Cot}\}Fe(CO)_2PPh_3]$ (4b): EI-MS: m/z (%): 608 (0.02) $[M^+ - 2CO]$, 403 (0.1) $[M^+ - PPh_3]$, 347 (2) $[M^+ - PPh_3 - 2CO]$, 291 (27) $[(Cp^*CrCot)^+]$, 262 (100) $[(PPh_3)^+]$, 187 (59) $[(Cp^*Cr)^+]$, 185 (93) $[(PPh_2)^+]$, 133 (23), 119 (20), 108 (56) $[(PPh)^+]$, 104 (13) $[Cot^+]$, 77 (15) $[Ph^+]$, 65 (6) $[Cp^+]$, 52 (82) $[Cr^+]$; $C_{38}H_{38}CrFeO_2P$ (665.54); calcd C 68.58, H 5.67; found C 68.73, H 5.71.

$[(C_5Me_5)Cr\{\mu\text{-}\eta^5(Cr)\text{:}\eta^3(Fe)\text{-Cot}\}Fe(CO)_2P(OEt)_3]$ (4c): EI-MS: m/z (%): 569 (3.7) $[M^+]$, 513 (2) $[M^+ - 2CO]$, 347 (49) $[M^+ - P(OEt)_3]$, 319 (8) $[M^+ - P(OEt)_3 - CO]$, 291 (13) $[M^+ - P(OEt)_3 - 2CO$ and $(Cp^*CrCot)^+]$, 187 (21) $[(Cp^*Cr)^+]$, 166 (34) $[\{P(OEt)_3\}^+]$, 133 (11), 119 (40), 104 (59) $[Cot^+]$, 65 (100) $[Cp^+]$, 52 (23) $[Cr^+]$; found and calculated isotopic distribution of M^+ (m/z values are normalized to m/z = 569 (58%)): m/z (found%, calcd%) = 567 (5, 6.6), 568 (2, 2.4), 569 (58, 57.5), 570 (23, 24.6), 571 (6, 7.2), 572 (1, 1.4).
$C_{26}H_{38}CrFeO_5P$ (569.41): calcd C 54.84, H 6.73; found C 54.60, H 6.65.

$[(C_5Me_5)Cr\{\mu\text{-}\eta^5(Cr)\text{:}\eta^3(Fe)\text{-Cot}\}Fe(CO)_2PF_3]$ (4d): PF_3 was slowly passed through a capillary into the reaction vessel, which was secured by a valve that prevented the entry of air, and released the overpressure in the reaction vessel. Unreacted PF_3 was destroyed by bubbling it through concentrated H_2SO_4. IR spectra were recorded periodically to monitor the progress of the reaction. After 3 h no $\tilde{\nu}$(CO) bands of the starting material **2** could be recorded (workup procedure, vide supra). EI-MS: m/z (%): 491 (0.6) $[M^+]$, 463 (0.2) $[M^+ - CO]$, 403 (6) $[M^+ - PF_3]$, 375 (7) $[M^+ - PF_3 - CO]$, 347 (40) $[M^+ - PF_3 - 2CO]$, 291 (59) $[(Cp^*CrCot)^+]$, 187 (100) $[(Cp^*Cr)^+]$, 133 (30), 119 (28), 104 (24) $[Cot^+]$, 88 (29) $[(PF_3)^+]$, 78 (20), 69 (30) $[(PF_2)^+]$, 52 (86) $[Cr^+]$; $C_{20}H_{23}CrF_3FeO_2P$ (491.22); calcd C 48.90, H 4.72, found C 48.32, H 4.80.

Crystal Structure Analyses: The measurements were performed in a Hilger & Watts (Y290), applying monochromatic $Mo_{K\alpha}$ radiation. The heavy atoms were found by direct methods using SHELXS86.[27] The structures were refined using SHELXL92[28] or SHELXL93.[29] See Table 7 for more details concerning the crystal data and data collection.[30]

Table 7. Crystal data and results of structure analysis.

	2	**3a**	**4c**
formula	$C_{21}H_{23}CrFeO$	$C_{18}H_{22}O_2CrFeO_2P$	$C_{26}H_{38}CrFeO_5P$
M_r	431.24	409.18	569.38
crystal size (mm^3)	$0.2\times0.2\times0.4$	$0.3\times0.3\times0.4$	$0.2\times0.2\times0.4$
crystal system	monoclinic	tetragonal	monoclinic
space group	$P2_1/n$	$P4_2/n$	$P2_1/c$
a (pm)	997.7(5)	2291.2(4)	1781.1(10)
b (pm)	1342.3(6)	–	1030.1(2)
c (pm)	1450.8(11)	679.1(1)	1608.9(5)
β [°]	104.53(5)	–	115.29(3)
V [nm^3]	1.881(2)	3.565(1)	2.669(2)
Z	4	8	4
radiation (pm)	71.073	71.073	71.073
ρ_{calcd} ($g\,cm^{-3}$)	1.523	1.525	1.417
abs. coeff μ (mm^{-1})	1.360	1.518	1.044
T (K)	153	153	153
scan type	ω-2θ	ω-2θ	ω-2θ
scan range	$2.6\le2\theta\le25.0$	$2.5\le2\theta\le25.0$	$2.5\le2\theta\le27.5$
range in hkl	$-1\le h\le11$	$0\le h\le27$	$-21\le h\le20$
	$-1\le k\le15$	$-1\le k\le17$	$-13\le k\le1$
	$-17\le l\le17$	$-1\le l\le8$	$-1\le l\le19$
total no. refl.	4446	3442	7494
no independ refl.	3327	3159	6057
data/restraints/parameter	3327/0/242	3159/0/311	6057/0/311
goodness-of-fit on F^2	0.870	0.834	1.048
R_1 [$I>2\sigma(I)$]	0.0541	0.0332	0.0492
ωR_2 [$I>2\sigma(I)$]	0.1410	0.0771	0.1204
R_1 (all data)	0.0678	0.0541	0.0686
ωR_2 (all data)	0.1563	0.0896	0.1323
largest diff. peak, hole [$e\,nm^{-3}$]	1047, −1155	492, −346	720, −676

Acknowledgements: This work was partly supported by the Netherlands Foundation for Chemical Research (SON) with financial aid from the Netherlands Organization for Scientific Research (NWO) (H. C. B.).

Supplementary material: Calculated spectra of the solution ESR spectra of **2**, **4b**, and **4d** and of the solid-solution ESR spectra of **4b** and **4d** (5 pages) are available from the author.

Received: December 12, 1996 [F 554]

[1] J. Heck, P. M. J. A. Hermans, A. B. Scholten, W. P. J. H. Bosman, G. Meyer, T. Staffel, R. Stürmer, M. Wünsch, *Z. Anorg. Allg. Chem.* **1992**, *611*, 35–42.
[2] P. M. J. A. Hermans, A. B. Scholten, E. K. van den Beuken, H. C. Brussaard, A. Roclofsen, B. Metz, E. J. Reijerse, P. T. Beurskens, W. P. Bosman, J. M. M. Smits, J. Heck, *Chem. Ber.* **1993**, *126*, 553–563.
[3] W. Fu, R. McDonald, J. Takats, A. H. Bond, R. D. Rogers, *Inorg. Chim. Acta* **1995**, *229*, 307–313.
[4] J. H. Bieri, T. Egolf, W. von Philipsborn, U. Piantini, R. Prewo, U. Ruppli, A. Salzer, *Organometallics*, **1986**, *5*, 2413–2425.
[5] H. Wadepohl, W. Galm, H. Pritzkow, *Angew. Chem.* **1990**, *102*, 701–703; *Angew. Chem. Int. Ed. Engl.* **1990**, *29*, 686–688.
[6] C. Bonifaci, A. Ceccon, A. Gambaro, P. Ganis, S. Santi, A. Venzo, *Organometallics* **1995**, *14*, 2430–2434.
[7] J. Heck, G. Rist, *J. Organomet. Chem.* **1988**, *342*, 45–65.
[8] H. Fleckner, F. W. Grevels, D. Hess, *J. Am. Chem. Soc.* **1984**, *106*, 2027–2032.
[9] M. Bigorgne, *J. Organomet. Chem.* **1970**, *34*, 211–229; R. L. Keiter, E. A. Keiter, K. H. Hecker, C. A. Boecker, *Organometallics* **1988**, *7*, 2466–2469; Y.-M. Wuu, J. G. Bentsen, C. G. Brinkley, M. S. Wrighton, *Inorg. Chem.* **1987**, *26*, 530–540.
[10] J. W. Freeman, N. C. Hallinan, A. M. Arif, R. W. Gedrige, R. D. Ernst, F. Basolo, *J. Am. Chem. Soc.* **1991**, *113*, 6509–6520; R. D. Ernst, *Chem. Rev.* **1988**, *88*, 1255–1294.
[11] C. F. Putnik, J. J. Welter, G. D. Stucky, M. J. D'Aniello, Jr., B. A. Sosinsky, J. F. Kirner, E. L. Muetterties, *J. Am. Chem. Soc.* **1978**, *100*, 4107–4116.
[12] M. Airoldi, G. Deganello, G. Gennaro, M. Moret, A. Sironi, *J. Chem. Soc. Chem. Commun.* **1992**, 850–851; R. G. Ball, F. Edelmann, G-Y. Kiel, J. Takats, R. Drews, *Organometallics*, **1986**, *5*, 829–839.
[13] W. A. Herrmann, J. Rohrmann, E. Herdtweck, C. Hecht, M. L. Ziegler, O. Serhadli, *J. Organomet. Chem.* **1986**, *314*, 295–305.
[14] R. D. Adams, D. M. Collins, F. A. Cotton, *Inorg. Chem.* **1974**, *13*, 1086–1090.

[15] a) D. W. Clack, W. Smith, *Inorg. Chim. Acta* **1976**, *20*, 93–97; b) C. Elschenbroich, F. Gerson, F. Stohler, *J. Am. Chem. Soc.* **1973**, *95*, 6956–6961.
[16] M. Symons, *Chemical and Biochemical Aspects of Electron-Spin Resonance Spectroscopy*, Van Nostrand Reinhold Company, N. Y, **1978**, p. 26ff,
[17] K. Angermund, P. Betz, A. Döhring, P. W. Jolly, C. Krüger, K. U. Schönfelder, *Polyhedron*, **1993**, *12*, 2663–2669.
[18] E. L. Muetterties, B. A. Sosinsky, K. I. Zamaraev, *J. Am. Chem. Soc.* **1975**, *97*, 5299–5300.
[19] C. A. Goulin, M. C. Baird, *Inorg. Chem. Acta.* **1990**, *168*, 195–199.
[20] N. Van Order, Jr., W. E. Geiger, T. E. Bitterwolf, A. L. Rheingold, *J. Am. Chem. Soc.* **1987**, *109*, 5680–5690; F. G. Herring, P. Legzdins, W. S. McNeil, M. J. Shaw, *ibid.* **1991**, *113*, 7049–7050; S. Fortier, M. C. Baird, K. F. Preston, J. R. Morton, T. Ziegler, T. J. Jaeger, W. C. Watkins, J. H. MacNeil, K. A. Watson, K. Hensel, Y. Le Page, J.-P. Charland, A. J. Williams, *ibid.* **1991**, *113*, 542–551.
[21] D. G. Gilheany, *Chem. Rev.* **1994**, *94*, 1339–1374; A. G. Orpen, N. Connelly, *J. Chem. Soc. Chem. Commun.* **1985**, 1310–1311.
[22] G. Pacchioni, P. S. Bagus, *Inorg. Chem.* **1992**, *31*, 4391–4398.
[23] B. Bachmann, J. Heck, *Organometallics* **1991**, *10* ,1373–1376.
[24] a) C. Elschenbroich, M. Nowotny, B. Metz, W. Massa, J. Graulich, *Angew. Chem.* **1991**, *103*, 601–604; *Angew. Chem. Int. Ed. Engl.* **1991**, *30*, 547–551; C. Elschenbroich, F. Bär, E. Bilger, D. Mahrwald, M. Nowotny, B. Metz; *Organometallics*, **1993**, *12*, 3373–3378; b) C. Elschenbroich, E. Bilger, B. Metz; *ibid.* **1991**, *10*, 2823–2827; E. Bilger, *Dissertation*, **1984**, Marburg.
[25] D. Astruc, *Comments Inorg. Chem.* **1987**, *6*, 61–84; D. Astruc, *Chem. Rev.* **1988**, *88*, 1189–1216; U. Kölle, F. Kouzami, *Angew. Chem.* **1980**, *92*, 658–659; *Angew. Chem. Int. Ed. Engl.* **1980**, *19*, 640–643.
[26] W. E. Geiger, A. Salzer, J. Edwin, W. von Philipsborn, U. Piantini, A. L. Rheingold, *J. Am. Chem. Soc.* **1990**, *112*, 7113–7121.
[27] G. M. Sheldrick, *SHELXS-86*, Universität Göttingen **1986**.
[28] G. M. Sheldrick, *SHELXL-92* Universität Göttingen **1992**.
[29] G. M. Sheldrick, *SHELXL-93*, Universität Göttingen **1993**.
[30] Crystallographic data (excluding structure factors) for the structures reported in this paper have been deposited with the Cambridge Crystallographic Data Centre as supplementary publication No. CCDC-100218. Copies of the data can be obtained free for charge on application to The Director, CCDC, 12 Union Road, Cambridge CB21EZ, UK (Fax: Int. code +(1223)336-033; e-mail: deposit@chemcrys.cam.ac.uk).